Journal of Alloys and Compounds 513 (2012) 304–309

Contents lists available at SciVerse ScienceDirect

Journal of Alloys and Compounds

journal homepage: www.elsevier.com/locate/jallcom

Subsolidus phase relations of the SrO–WO_3–CuO system at 800 °C in air

J.-C. Grivel*, P. Norby

Materials Research Division, Risø National Laboratory for Sustainable Energy, Technical University of Denmark, Frederiksborgvej 399, DK 4000 Roskilde, Denmark

ARTICLE INFO

Article history:
Received 15 August 2011
Received in revised form 31 August 2011
Accepted 2 September 2011
Available online 24 October 2011

Keywords:
Phase equilibria
X-ray diffraction
SrO–WO_3–CuO

ABSTRACT

The subsolidus phase relations of the SrO–WO_3–CuO system were investigated in air. The samples were equilibrated at 800 °C. Under these conditions, eight binary oxides are stable. The pseudo-ternary section contains two ternary oxide phases: the previously described Sr_2CuWO_6 phase as well as a new phase with $Sr_8CuW_3O_{18}$ stoichiometry. The crystal structure of this new compound was solved and refined in the *R*-3 space group, unit cell parameters $a = 5.7202$ Å and $c = 28.873$ Å. $Sr_8CuW_3O_{18}$ has a distorted perovskite type structure, where some of the Sr atoms are positioned at the B sites, and the composition may be given as: $Sr_6(Sr_2CuW_3)O_{18}$. There are indications of existence of a superstructure or stacking faults related to Cu/Sr ordering.

1. Introduction

Following the discovery of the $YBa_2Cu_3O_7$ high-temperature superconductor [1] and owing to the fact that most lanthanide elements can be substituted in its structure, the phase equilibria of the pseudo-ternary BaO–RE_2O_3–CuO systems (with RE = rare earth) have been widely investigated ([2] and references therein). More recently, the subsolidus phase relationships of all SrO–RE_xO_y–CuO systems have been determined, unveiling a rich variety of compounds, especially for the light rare-earth elements [3–17]. In contrast, only few SrO–MO_x–CuO pseudo-ternary systems involving transition metal elements (M) have been studied in details until now. In air at 900 °C, only one ternary oxide compound was found for the IVB group elements [18]. Studies devoted to systems involving elements from the VB group revealed the existence of several ternary oxides (SrV_2CuO_7, $Sr_3Nb_2CuO_9$ and $Sr_3Ta_2CuO_9$) as well as several ternary solid solutions [19–22]. Finally, in the SrO–Fe_2O_3–CuO system, a new ternary oxide compound with $Sr_7Fe_{17}CuO_{34}$ composition was evidenced by Yang et al. [23].

The phase equilibria of the SrO–MO_x–CuO systems where M is an element of the VIB transition metals group are only sparsely known. To the best of our knowledge, only one ternary oxide compound (Sr_2WCuO_6 [24]) has been reported to form in these combinations of elements up to now. The present study is a contribution towards a better knowledge of the chemistry of these systems.

1.1. Previous work

At ambient pressure, WO_3 adopts various structural modifications depending on temperature. In the 300–850 °C range, it crystallises in the $P2_1/n$ space group (monoclinic) [25].

Several studies [26–32] have been devoted to the SrO–CuO system, in which three phases are known to be stable at 800 °C in air: Sr_2CuO_3 (orthorhombic, space group *Immm* [33]), $SrCuO_2$ (orthorhombic, space group *Cmcm* [33]) and $Sr_{14}Cu_{24}O_{41}$ (sometimes described as $Sr_3Cu_5O_8$) (orthorhombic, space group *Fmmm* [34]). Under conditions of lower oxygen partial pressure, an additional binary oxide with $SrCu_2O_2$ composition was observed [32,35]. The $SrCu_2O_3$ and $Sr_2Cu_3O_5$ phases were synthesised under high pressure (1.7–8 GPa) [36].

The WO_3–CuO system was first studied by Gebert and Kihlborg [37], who identified two intermediate phases after equilibrating reagent mixtures at 800 °C in sealed evacuated platinum tubes. These phases are Cu_3WO_6 (cubic, space group *Pa*-3 [38]) and $CuWO_{4-x}$ (triclinic, space group *P*-1 [37]). The stoichiometry of the latter phase, which might be Cu-deficient, was not completely elucidated in Ref. [37]. More recently, Kol'tsova and Nipan [39] established the phase equilibria of the same system in air between 700 °C and 1000 °C. They report the existence of two binary oxides: Cu_3WO_6 and $CuWO_4$ (triclinic, space group *P*-1 [40]) that are stable at 800 °C. Another compound, Cu_2WO_4 was synthesised under reducing conditions [41]. Its structure has been determined by Marinder et al. [42] (triclinic, space group *P*1).

The phase equilibria in the SrO–WO_3 system were reported by Chang et al. [43] and later by Tokunov and Kislyakov [44]. According to the first study, $SrWO_4$ (tetragonal, space group $I4_1/a$ [45]) and Sr_3WO_6 (monoclinic, space group Cc [46]) phases are the only binary oxide phases present in the system at 800 °C [43], an

---

* Corresponding author. Tel.: +45 4677 4739; fax: +45 4677 5758.
E-mail addresses: jean@risoe.dtu.dk, jean-claude.grivel@risoe.dk (J.-C. Grivel).

0925-8388/$ – see front matter © 2011 Elsevier B.V. All rights reserved.
doi:10.1016/j.jallcom.2011.09.104

additional phase (Sr_2WO_5 orthorhombic, space group *Pmnb* [47]) was found to be stable at this temperature in the second study [44].

In the SrO–WO_3–CuO system, Kapshev et al. [24] reported on the synthesis of a $CuSr_2WO_6$ ternary oxide phase. Its structure was further refined by Reinen and Weitzel [48] (tetragonal, space group *I*4/*m*).

2. Experimental details

High purity WO_3, $SrCO_3$ and CuO, powders (all ≥99.9%) were thoroughly mixed in an agate mortar and calcined at 800 °C for 60 h. In total, 71 nominal compositions were studied. After grinding, pellets were pressed under a pressure of 1.8 kbar and sintered at least twice at 800 °C for 60 h with intermediate grinding and repressing. The samples were air-quenched at the end of the sintering treatments. All heat treatments were performed in air.

The phase content of the pellets was checked after each heat treatment by X-ray diffraction (XRD) in a STOE diffractometer using CuKα radiation. In some cases, additional heat treatments were performed in order to reach equilibrium. Equilibrium was considered as achieved if no differences were detectable in the XRD patterns performed after two consecutive sintering treatments. Silicon powder was added as an internal standard for lattice parameter determination in selected samples. In the case of $CuWO_4$, for which too severe overlap with the Si reflections takes place, annealed KCl powder was used as a standard instead of Si.

High-resolution synchrotron X-ray powder diffraction data for structure determination of $Sr_8CuW_3O_{18}$ were collected at beamline 11-BM at the Advanced Photon Source (APS), Argonne National Laboratory [49–51]. The sample was packed into a 0.8 mm Kapton capillary. A wavelength of 0.41315 Å was used and data were collected using discrete detectors covering an angular range from $-6°$ to $16°$ 2θ, which were scanned over a $34°$ 2θ range. Data points were collected every $0.001°$ 2θ using a scan speed of $0.01°/s$, but were merged to a step size of $0.002°$ in 2θ in order to better fit the peak widths of the reflections. Data from $2°$ to $40°$ in 2θ were used. The crystal structure was solved using FOX [52] and subsequent Rietveld refinement using GSAS (expgui) [53,54] was used to assign the atoms.

3. Results and discussion

3.1. SrO–CuO

Three binary oxide phases were formed at 900 °C in air: Sr_2CuO_3, $SrCuO_2$ and $Sr_{14}Cu_{24}O_{41}$, in agreement with previous reports [26–32]. The $SrCu_2O_2$ phase was not found in the present study as a consequence of the lack of stability of this phase in air [32,35]. The high-pressure phases $SrCu_2O_3$ and $Sr_2Cu_3O_5$ [36] were not formed either.

3.2. WO_3–CuO

In agreement with the results presented in Ref. [39], $CuWO_4$ and Cu_3WO_6 are the only binary oxide phases stable at 800 °C in air in this system. The detection of Cu_3WO_6 in the sample with $Cu_{0.99}W_{0.01}O_x$ nominal composition, coupled with similar CuO lattice parameters (Table 1) allows concluding that no extended substitution of W occurs in CuO under the present experimental conditions. Similarly (presence of $CuWO_4$ and equivalent lattice parameters – Table 1) show that Cu substitution in WO_3 is in any case limited to less than 1 at.%. As shown in Table 1, departing from the ideal $CuWO_4$ and Cu_3WO_6 compositions results in equilibrium between the respective stoichiometric phases and other compounds. $CuWO_4$ and Cu_3WO_6 thus do not appear to form solid solutions, as previously reported in Ref. [39].

3.3. WO_3–SrO

In this pseudo-binary system, we found 3 stable binary oxides with compositions $SrWO_4$, Sr_2WO_5 and Sr_3WO_6. Excess SrO or WO_3 in the respective starting compositions for these phases systematically results in the appearance of impurities, while the cell parameters of the main phases are not affected. Similar considerations are valid for the WO_3 and SrO end compounds except that the SrO phase in the samples with SrO and $Sr_{0.99}W_{0.01}O_x$ nominal compositions was too unstable under ambient conditions, due to reaction with water, to allow reliable cell parameter determinations. None of these phases appears to form extended solid solutions and our results are therefore in agreement with the data published in Ref. [44].

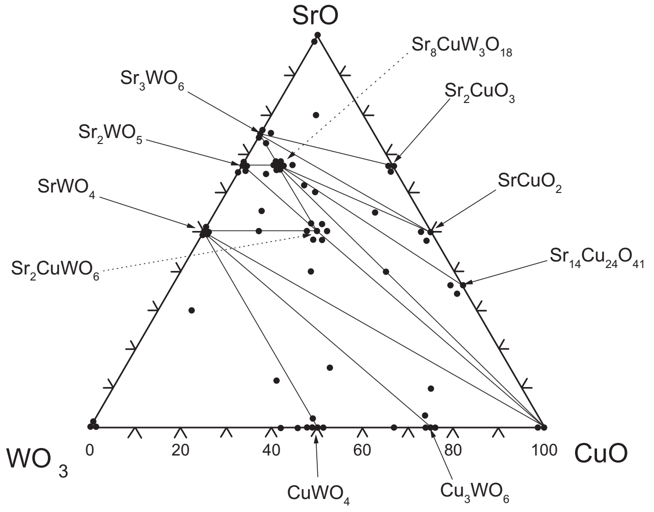

Fig. 1. Phase equilibria of the SrO–WO_3–CuO system at 800 °C in air. Dots represent the studied compositions.

3.4. SrO–WO_3–CuO

The tie-line compatibilities of phases in the pseudo-ternary SrO–WO_3–CuO phase diagram at 800 °C in air are shown in Fig. 1. There are 8 binary oxide phases, 2 ternary oxide phases and 13 three-phase regions. None of the binary oxide phases of the pseudo-binary systems appear to give rise to ternary solid solutions as can be deduced from the appearance of 2-phase or 3-phase equilibria when attempts were made to dope these compounds with the third element (Table 1). The $CuSr_2WO_6$ phase [24] appears to have no extended solubility range as shown by the appearance of secondary phases as soon as the nominal composition departs from the ideal stoichiometry and the fact that the lattice parameters of $CuSr_2WO_6$ are not affected by slight modifications of the overall composition of the sample (Table 1). In addition, a new ternary oxide phase with $Sr_8W_3CuO_{18}$ composition was found in the Sr-rich area of the pseudo-ternary phase diagram. This phase does not appear to form a solid solution either.

3.5. The $Sr_8W_3CuO_{18}$ phase

The powder diffraction pattern was indexed based on a rhombohedral unit cell (refined unit cell parameters $a = 5.7202$ Å and $c = 28.8731$ Å). Systematic extinctions were in agreement with the space groups *R*-3, *R*-3*m*, *R*3, *R*3*m*, *R*32. The crystal structure was solved using the space group *R*-3*m*, which gave the positions of all atoms. The Rietveld refinement indicated that the space group was not correct, and the final refinement of the structure was done in the space group *R*-3. Fig. 2 shows observed, calculated and difference powder diffraction patterns. Table 2 gives the refined coordinates, while Table 3 gives some of the relevant bond distances in the structure.

An impurity of Sr_2WO_5 was observed (~0.5 wt% according to the Rietveld refinement). Excluded regions were used in order to omit some additional weak reflections, which could not be indexed. One low angle reflection at $d = 19.282$ Å could not be indexed based on this unit cell. However, the *d*-value is twice that of the 0 0 3

Table 1
Phases observed in selected samples after equilibration and crystallographic data for the majority phases.

Nominal cation ratio	Phases (XRD)[a]	Space group[b]	Lattice parameters[c]					
W:Sr:Cu			*a* [Å]	*b* [Å]	*c* [Å]	α [°]	β [°]	γ [°]
0:0:100	CuO	$C2/c$	4.663 (8)	3.416 (2)	5.136 (11)	–	99.50 (3)	–
1:0:99	CuO (Cu_3WO_6)	$C2/c$	4.661 (8)	3.416 (2)	5.138 (11)	–	99.52 (3)	–
24:0:76	Cu_3WO_6 (CuO)	*Pa*-3	9.776 (2)	–	–	–	–	–
25:0:75	Cu_3WO_6	*Pa*-3	9.782 (2)	–	–	–	–	–
26:0:74	Cu_3WO_6 ($CuWO_4$)	*Pa*-3	9.800 (2)	–	–	–	–	
25:3:72	Cu_3WO_6 (CuO, $SrWO_{4)}$	*Pa*-3	9.778 (2)	–	–	–	–	–
49:0:51	$CuWO_4$ (Cu_3WO_6)	*P*-1	4.706 (3)	5.845 (3)	4.881 (3)	91.64 (5)	92.43 (6)	82.75 (6)
50:0:50	$CuWO_4$	*P*-1	4.705 (3)	5.843 (3)	4.879 (2)	91.65 (4)	92.44 (5)	82.78 (5)
51:0:49	$CuWO_4$ (WO_3)	*P*-1	4.706 (3)	5.844 (3)	4.881 (2)	91.68 (4)	92.41 (5)	82.77 (5)
50:2:48	$CuWO_4$ ($SrWO_4$)	*P*-1	4.706 (3)	5.843 (3)	4.880 (3)	91.65 (4)	92.42 (5)	82.78 (5)
99:0:1	WO_3 ($CuWO_4$)	$P2_1/n$	7.289 (3)	7.525 (3)	7.669 (5)	–	90.94 (5)	–
100:0:0	WO_3	$P2_1/n$	7.293 (3)	7.528 (3)	7.669 (5)	–	90.93 (5)	–
99:1:0	WO_3 ($SrWO_4$)	$P2_1/n$	7.291 (3)	7.530 (3)	7.672 (5)	–	90.94 (4)	–
51:49:0	$SrWO_4$ (WO_3)	$I4_1/a$	5.405 (2)	–	11.925 (7) –	–	–	
50:50:0	$SrWO_4$	$I4_1/a$	5.407 (2)	–	11.926 (6) –	–	–	
49:51:0	$SrWO_4$ (Sr_2WO_5)	$I4_1/a$	5.406 (2)	–	11.925 (7)	–	–	–
48.75:50:1.25	$SrWO_4$ (Sr_2CuWO_6)	$I4_1/a$	5.408 (2)	–	11.926 (5)	–	–	–
50:48.75:1.25	$SrWO_4$ ($CuWO_4$)	$I4_1/a$	5.407 (2)	–	11.930 (5)	–	–	–
35:65:0	Sr_2WO_5 ($SrWO_4$)	*Pnam*	7.235 (4)	10.861 (7)	5.537 (2)	–	–	–
1/3:2/3:0	Sr_2WO_5	*Pnam*	7.231 (4)	10.861 (7)	5.534 (2)	–	–	–
32:68:0	Sr_2WO_5 (Sr_3WO_6)	*Pnam*	7.237 (3)	10.862 (6)	5.535 (2)	–	–	–
31.67:66.67:1.67	Sr_2WO_5 ($Sr_8CuW_3O_{15}$)	*Pnam*	7.235 (3)	10.862 (6)	5.535 (2)	–	–	–
33.33:65.00:1.67	Sr_2WO_5 (Sr_3CuWO_6, $SrWO_4$)	*Pnam*	7.238 (3)	10.865 (5)	5.538 (2)	–	–	–
26:74:0	Sr_3WO_6 (Sr_2WO_5)		8.353 (6)	8.290 (6)	8.202 (5)	89.75 (32)	89.89 (13)	89.57 (13)
25:75:0	Sr_3WO_6		8.350 (4)	8.286 (4)	8.198 (4)	89.93 (21)	89.86 (8)	89.69 (8)
24:76:0	Sr_3WO_6 (SrO)		8.352 (8)	8.283 (8)	8.203 (7)	89.79 (44)	89.90 (17)	89.70 (17)
23:75:2	Sr_3WO_6 (SrO, Sr_2CuO_3)		8.352 (4)	8.288 (4)	8.210 (4)	89.89 (22)	89.86 (8)	89.64 (9)
25:73:2	Sr_3WO_6 ($SrCuO_2$, $Sr_8W_3CuO_{18}$)		8.351 (5)	8.286 (5)	8.202 (5)	89.64 (28)	89.89 (11)	89.66 (11)
1.67:66.67:31.67	Sr_2CuO_3 (Sr_3WO_6, $SrCuO_2$)	*Immm*	12.690 (3)	3.907 (1)	3.495 (2)	–	–	–
0.00:66.67:33.33	Sr_2CuO_3	*Immm*	12.683 (3)	3.906 (1)	3.492 (2)	–	–	–
1.67:65.00:33.33	Sr_2CuO_3 (Sr_3WO_6, $SrCuO_2$)	*Immm*	12.689 (3)	3.907 (1)	3.495 (1)	–	–	–
2.5:50:47.5	$SrCuO_2$ ($Sr_8CuW_3O_{18}$, $Sr_{14}Cu_{24}O_{41}$)	*Cmcm*	3.563 (3)	16.295 (6)	3.904 (4)	–	–	–
0:50:50	$SrCuO_2$	*Cmcm*	3.563 (2)	16.287 (3)	3.903 (2)	–	–	–
2.5:47.5:50	$SrCuO_2$ ($Sr_8CuW_3O_{18}$, $Sr_{14}Cu_{24}O_{41}$)	*Cmcm*	3.562 (3)	16.299 (6)	3.903 (4)	–	–	–
1.0:14.0:23.0	$Sr_{14}Cu_{24}O_{41}$ (CuO, $Sr_8CuW_3O_{18}$)	*Cccm*	11.444 (2)	13.368 (2)	3.950 (2)	–	–	–
0.0:14.0:24.0	$Sr_{14}Cu_{24}O_{41}$	*Cccm*	11.452 (4)	13.374 (4)	3.946 (3)	–	–	–
1.0:13.0:24.0	$Sr_{14}Cu_{24}O_{41}$ (CuO, $Sr_8CuW_3O_{18}$)	*Cccm*	11.450 (5)	13.369 (5)	3.949 (3)	–	–	–
25:50:25	Sr_2CuWO_6	$I4/m$	5.419 (2)	–	8.398 (3)	–	–	–
25:52:23	Sr_2CuWO_6 ($Sr_8W_3CuO_{18}$)	$I4/m$	5.417 (1)	–	8.396 (3)	–	–	–
23:52:25	Sr_2CuWO_6 ($Sr_8W_3CuO_{18}$, CuO)	$I4/m$	5.421 (1)	–	8.395 (2)	–	–	–
27:50:23	Sr_2CuWO_6 ($SrWO_4$)	$I4/m$	5.423 (2)	–	8.394 (2)	–	–	–
23:50:27	Sr_2CuWO_6 ($Sr_8W_3CuO_{18}$, CuO)	$I4/m$	5.418 (2)	–	8.394 (3)	–	–	–
27:48:25	Sr_2CuWO_6 ($SrWO_4$, CuO)	$I4/m$	5.420 (2)	–	8.397 (3)	–	–	–
25:48:27	Sr_2CuWO_6 ($SrWO_4$, CuO)	$I4/m$	5.421 (1)	–	8.393 (1)	–	–	–
25.00:66.67:8.33	$Sr_8CuW_3O_{18}$	*R*-3	5.721 (4)	–	28.87 (4)	–	–	–
25.00:67.50:7.50	$Sr_8CuW_3O_{18}$ (Sr_3WO_6)	*R*-3	5.720 (3)	–	28.89 (2)	–	–	–
24.00:67.50:8.50	$Sr_8CuW_3O_{18}$ (Sr_3WO_6, $SrCuO_2$)	*R*-3	5.721 (3)	–	28.88 (2)	–	–	–
24.17:66.67:9.17	$Sr_8CuW_3O_{18}$ (Sr_3WO_6, $SrCuO_2$)	*R*-3	5.719 (2)	–	28.86 (2)	–	–	–
25.00:65.50:9.50	$Sr_8CuW_3O_{18}$ (CuO)	*R*-3	5.720 (3)	–	28.89 (2)	–	–	–
26.00:65.50:8.50	$Sr_8CuW_3O_{18}$ (Sr_2CuWO_6, Sr_2WO_5)	*R*-3	5.720 (3)	–	28.90 (2)	–	–	–
25.83:66.67:7.50	$Sr_8CuW_3O_{18}$ (Sr_2WO_5)	*R*-3	5.719 (2)	–	28.88 (2)	–	–	–

[a] Phases between brackets are minority phases.
[b] Space group of the majority phase.
[c] The lattice parameters are those of the majority phase.

reflection, indicating that the true unit cell may have a doubling of the *c*-axis possibly due to ordering of the copper atoms.

The unit cell and space group found for $Sr_8CuW_3O_{18}$ indicated a perovskite type structure, but with strontium occupying 1/3 of the 6-coordinated B sites. The 12-coordinated A-sites are occupied also with Sr, and the composition of the material may therefore be given as $Sr_6(Sr_2CuW_3)O_{18}$. The structure determination and refinement verified that the structure may indeed be described as a distorted perovskite with Sr/Cu having distorted six-coordination to oxygen. Fig. 3 shows a polyhedral representation of the structure, showing

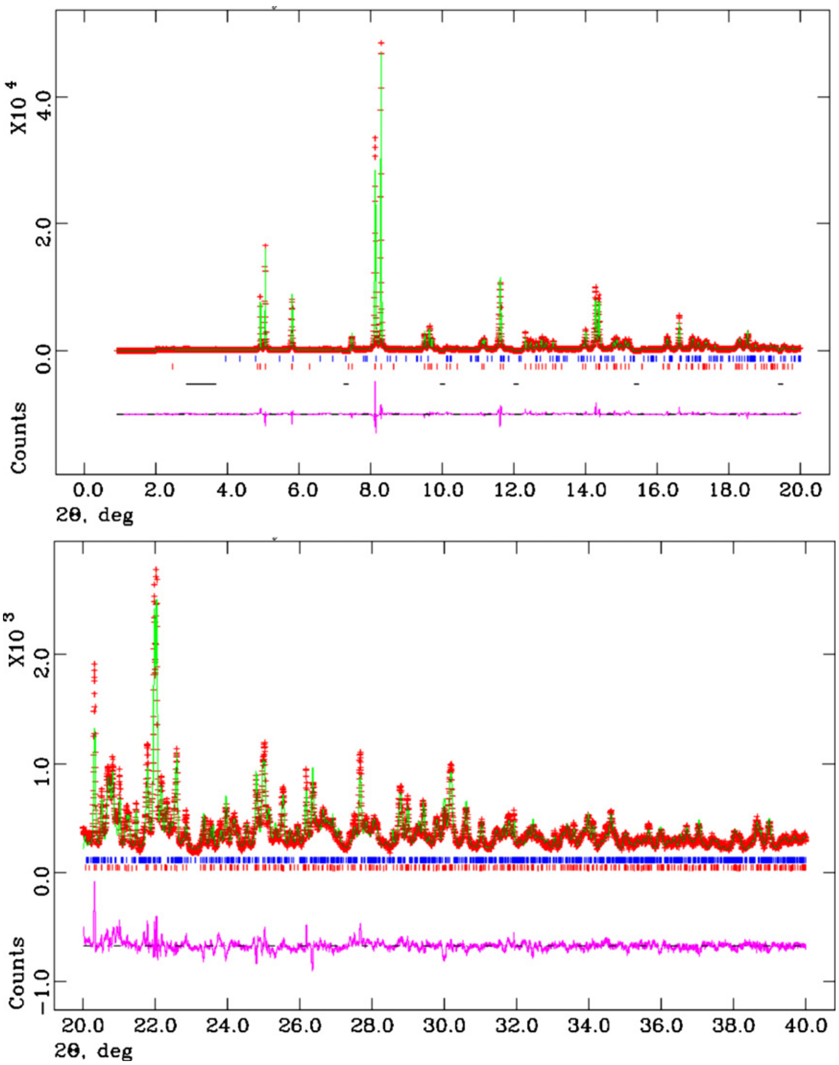

Fig. 2. Calculated, observed and difference powder diffraction profiles after Rietveld refinement of synchrotron X-ray powder diffraction data for $Sr_8CuW_3O_{18}$. The lower tic-marks (red) show the position of the reflections from the main phase, while the blue tic-marks represent the impurity phase (Sr_2WO_5, ~0.5 wt%). Excluded regions in the refinement are indicated by horizontal bars. (For interpretation of the references to color in this figure legend, the reader is referred to the web version of the article.)

only the B-site polyhedra. Tungsten forms fairly regular octahedra, while the Sr/Cu polyhedron is quite distorted with the central atom displaced from the center of gravity.

The refinement is not entirely satisfactory, indicating that, although the overall crystal structure is probably correct, the structure is not fully described with respect to the distribution of Sr and Cu on the B-sites, and possibly the anion arrangement. The challenges are related to the Cu/Sr position and the coordination around Sr1, which shows some quite short Sr-O distances (ca. 2.2 Å). The coordination requirements and bond distances to oxygen are quite different for Cu(II) and Sr. Therefore it is not surprising that a local variation in the structure occurs around these sites. This could reflect a statistic mixture of Cu and Sr, or, more probable, a superstructure as a result of Cu/Sr ordering. This could be described using a larger unit cell, lower symmetry or systematic stacking faults. The fact that the $Sr_6(Sr_2CuW_3)O_{18}$ phase does not appear to form solid solutions, may indicate an ordered distribution of Cu and Sr atoms, which is not taken into account in the presented structural model.

In the SrO–WO_3–CuO phase diagram, three perovskite-related phases with compositions WO_3 $(3-x)$SrO xCuO ($x = 1$, 1/3 and 0) are found: Sr_2CuWO_6 [24,55,56], $Sr_8CuW_3O_{18}$ (present work) and Sr_3WO_6 [46]. Sr_2CuWO_6, is a double perovskite with an ordered

Table 2
Atomic coordinates from the Rietveld refinement of $Sr_8CuW_3O_{18}$ ($Sr_6Sr_2CuW_3O_{18}$). Refinement in space group *R*-3 (148), unit cell parameters *a*: 5.72020 (4) Å, *c*: 28.8727 (3) Å (standard deviations are underestimated by the Rietveld refinement). Reliability factors: R_P: 0.10, R_{wP}: 0.13, R_F^2 : 0.056.

Atom	Wyckoff	*x*	*y*	*z*	*U* × 100	Occupancy
Sr1	6c	0	0	0.88679 (8)	3.51 (7)	1
Sr2	6c	0	0	0.63273 (6)	1.32 (4)	1
W1	3b	0	0	0.5	−0.55 (3)	1
W2	3a	0	0	0	0.13 (3)	1
Cu/Sr	6c	0	0	0.23465 (7)	4.02 (6)	1/3 Cu, 2/3 Sr
O1	18f	0.8749 (18)	0.1966 (17)	0.03886 (20)	1.34 (20)	1
O2	18f	0.9958 (17)	0.2638 (17)	0.53489 (32)	3.00	1

Table 3
Selected-bond distances and angles in the refined crystal structure of $Sr_8CuW_3O_{18}$.

Sr1	O1	2.681 (6) Å (×3)		Sr2	O1	2.660 (9) Å (×3)	
	O2	2.208 (8) Å (×3)			O1	2.717 (6) Å (×3)	
	O2	3.310 (9) Å (×3)			O1	3.068 (9) Å (×3)	
	O2	3.657 (9) Å (×3)			O2	3.208 (9) Å (×3)	
W1	O2 1.825 (8) Å (×6)			W2	O1	1.960 (7) Å (×6)	
O2	W1	O2	87.5 (4)° (×6)	O1	W2	O1	89.5 (3)° (×6)
O2	W1	O2	92.5 (4)° (×6)	O1	W2	O1	90.5 (3)° (×6)
O2	W1	O2	180° (×3)	O1	W2	O1	180° (×3)
Sr/Cu	O1	2.438 (6) Å (×3)					
Sr/Cu	O2	2.316 (8) Å (×3)					
O1	Sr/Cu	O1	75.4 (2)° (×3)				
O1	Sr/Cu	O2	156.5 (3)° (×3)				
O1	Sr/Cu	O2	81.2 (3)° (×3)				
O1	Sr/Cu	O2	96.5 (3)° (×3)				
O2	Sr/Cu	O2	104.2 (3)° (×3)				

distribution of Cu and W on the B-sites (P3). Sr_3WO_6 (Sr_2SrWO_6) is an example of perovskite materials with Sr on both A- and B-sites. Sr_3WO_6 has several polymorphs depending on temperature, and is an example of a double perovskite with broken corner sharing connectivity of the octahedral framework [46], resulting in an increase of the coordination around the Sr B-cations from 6 to 7 and 8. This is a result of a large difference in ionic radii of the B-site atoms (0.58 Å) and low tolerance factor, t (0.89). For Sr_2CuWO_6, the difference in the ionic radii of the B-site cations is much smaller (0.13 Å) and the tolerance factor is closer to unity (0.97), and the structure is therefore closer to the ideal perovskite. In $Sr_8CuW_3O_{18}$ ($Sr_2[Sr_{2/3}Cu_{1/3}W]O_6$) ($t$ = 0.91) there are three types of B-cations with a mixture of large and small differences in ionic radii, which will complicate the structural arrangement. Analysis of thermal transformations and further investigations using TEM are under way in order to elucidate the true structure of $Sr_8CuW_3O_{18}$.

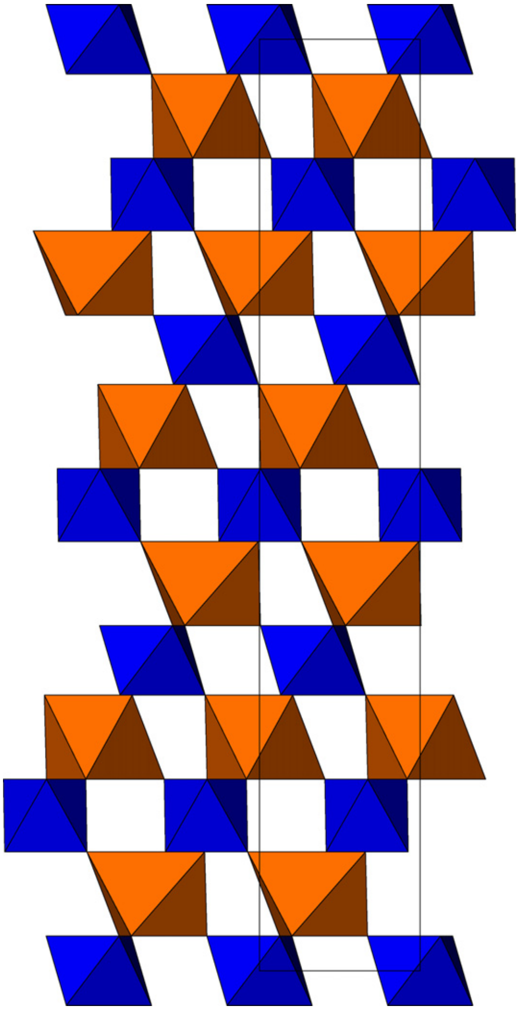

Fig. 3. The structure of $Sr_8CuW_3O_{18}$, showing the stacking sequence in the perovskite structure. Only the six-coordinated atoms are shown; W as blue and Sr/Cu as orange polyhedra. (For interpretation of the references to color in this figure legend, the reader is referred to the web version of the article.)

4. Conclusion

In air, at 800 °C, the SrO–WO_3–CuO system contains 13 three-phase regions, 8 binary oxide phases (Sr_2CuO_3, SrCuO, $Sr_{14}Cu_{24}O_{41}$, Cu_3WO_6, $CuWO_4$, $SrWO_4$, Sr_2WO_5 and Sr_3WO_6) and 2 ternary oxide phases with compositions Sr_2CuWO_6 and $Sr_8CuW_3O_{18}$. The latter, which is reported here for the first time, is an example of a double perovskite (with a mixture of three cations on the B-sites). Strontium is situated on both the A and B-site. The composition of the phase, which crystallises in the R-3 space group, with unit cell parameters a = 5.7202 Å and c = 28.873 Å may be given as $Sr_6(Sr_2CuW_3)O_{18}$. There are indications of the existence of a superstructure or stacking faults related to Cu/Sr ordering.

Acknowledgements

This work was financed by the Danish Ministry of Science, Technology and Innovation. Use of the Advanced Photon Source at Argonne National Laboratory was supported by the U.S. Department of Energy, Office of Science, Office of Basic Energy Sciences, under Contract No. DE-AC02-06CH11357.

References

[1] M.K. Wu, J.R. Ashburn, C.T. Torng, P.H. Hor, R.L. Meng, L. Gao, Z.J. Huang, Y.Q. Wang, C.W. Chu, Phys. Rev. Lett. 58 (1987) 908.
[2] W. Wong-Ng, B. Paretzkin, E.R. Fuller, J. Solid State Chem. 85 (1990) 117.
[3] D.M. De Leeuw, C.A.H.A. Mutsaers, G.P.J. Geelen, H.C.A. Smoorenburg, C. Langereis, Physica C 152 (1988) 508.
[4] F. Wu, S. Xie, Z. Che, J.K. Ling, J. Mater. Sci. 27 (1992) 3082.
[5] R.S. Roth, C.J. Rawn, J.D. Whitler, C.K. Chiang, W. Wong-Ng, J. Am. Ceram. Soc. 72 (1989) 395.
[6] D.M. De Leeuw, C.A.H.A. Mutsaers, G.P.J. Geelen, C. Langereis, J. Solid State Chem. 80 (1989) 276.
[7] X. Chen, J.K. Liang, C. Wang, G.H. Rao, X.R. Xing, Z.H. Song, Z.Y. Qiao, J. Alloys Compd. 205 (1994) 101.
[8] C.Q. Han, X.L. Chen, J.K. Liang, Q.L. Liu, G.H. Rao, J. Alloys Compd. 314 (2001) 301.
[9] C.Q. Han, X.L. Chen, J.K. Liang, Q.L. Liu, G.H. Rao, J. Solid State Chem. 156 (2001) 247.
[10] C.Q. Han, Y. Gao, X.L. Chen, J.K. Liang, G.H. Rao, J. Alloys Compd. 321 (2001) 54.
[11] W. Wong-Ng, Q. Huang, I. Levin, J.A. Kaduk, J. Dillingham, T. Haugan, J. Suh, L.P. Cook, Int. J. Inorg. Mater. 3 (2001) 1283.
[12] W. Wong-Ng, J. Dillingham, L.P. Cook, J. Solid State Chem. 149 (2000) 333.
[13] J.-C. Grivel, N.H. Andersen, J. Alloys Compd. 464 (2008) 457.

[14] C.Q. Han, X.L. Chen, J.K. Liang, Q.L. Liu, Y. Chen, G.H. Rao, J. Alloys Compd. 309 (2000) 95.
[15] J. Dillingham, W. Wong-Ng, I. Levin, Int. J. Inorg. Mater. 3 (2001) 569.
[16] J.-C. Grivel, N.H. Andersen, J. Alloys Compd. 391 (2005) 292.
[17] J.-C. Grivel, N.H. Andersen, J. Alloys Compd. 436 (2007) 261.
[18] J.-C. Grivel, J. Alloys Compd. 464 (2008) 457.
[19] V.D. Zhuravlev, Y.A. Velikodnyi, L.V. Kristallov, Zh. Neorg. Khim. 32 (1987) 3060.
[20] N.M. Drozdova, V.P. Sirotinkin, A.A. Evdokimov, Zh. Neorg. Khim. 36 (1991) 1588.
[21] V.P. Sirotinkin, N.M. Drozdova, Zh. Neorg. Khim. 36 (1993) 1791.
[22] J.-C. Grivel, J. Alloys Compd. 486 (2009) 293.
[23] L.T. Yang, J.K. Liang, G.B. Song, H. Chang, G.H. Rao, J. Alloys Compd. 353 (2003) 301.
[24] A. Kapshev, V. Ivanova, Yu. Venevtsev, Dokl. Akad. Nauk SSSR 167 (1966) 56.
[25] T. Vogt, P.M. Woodward, B.A. Hunter, J. Solid State Chem. 144 (1999) 209.
[26] J.K. Liang, C. Zhan, W. Fei, S.S. Xie, Solid State Commun. 75 (1990) 247.
[27] B.V. Slobodin, A.A. Fotiev, A.S. Kosmynin, G.E. Shter, I.K. Garkushin, V.L. Balashov, A.S. Trunin, Sverkhprovodimost: Fiz. Khim. Tekh. 3 (1990) 523.
[28] N.M. Hwang, R.S. Roth, C.J. Rawn, J. Am. Ceram. Soc. 73 (1990) 2531.
[29] A.K. Shirvinskaya, V.F. Popova, R.G. Grebenshchikov, Sverkhprovodimost: Fiz. Khim. Tekh. 3 (1990) 1872.
[30] R.O. Suzuki, P. Bohac, L.J. Gauckler, J. Am. Ceram. Soc. 75 (1992) 2833.
[31] M. Nevřiva, H. Kraus, Physica C 235–240 (1994) 325.
[32] C.B. Alcock, B.Z. Li, J. Am. Ceram. Soc. 73 (1990) 1176.
[33] M.T. Weller, M.T. Lines, J. Solid State Chem. 82 (1989) 21.
[34] E.M. McCarron, M.A. Subramanian, J.C. Calabrese, R.L. Harlow, Mater. Res. Bull. 23 (1988) 1355.
[35] C.L. Teske, H. Müller-Buschbaum, Z. Anorg. Allg. Chem. 379 (1970) 113.
[36] N. Kobayashi, Z. Hiroi, M. Takano, J. Solid State Chem. 132 (1997) 274.
[37] E. Gebert, L. Kihlborg, Acta Chem. Scand. 21 (1967) 2575.
[38] E. Gebert, L. Kihlborg, Acta Chem. Scand. 23 (1969) 221.
[39] T.N. Kol'tsova, G.N. Nipan, Inorg. Mater. 35 (1999) 383.
[40] L. Kihlborg, E. Gebert, Acta Cryst. B26 (1970) 1020.
[41] H. Haas, E. Kordes, Z. Kristallogr. 129 (1969) 252.
[42] B.O. Marinder, P.L. Wang, P.E. Werner, M. Westdahl, A.F. Andersen, D. Louer, Acta Chem. Scand. A 41 (1987) 152.
[43] L.L.Y. Chang, M.G. Scroger, B. Pjillips, J. Am. Ceram. Soc. 49 (1966) 385.
[44] O.I. Tokunov, I.P. Kislyakov, Izv. Vyssh. Uchebn. Zaved Khim. Tekhnol. 15 (1972) 1609.
[45] E. Gürmen, E. Daniels, J.S. King, J. Chem. Phys. 55 (1971) 1093.
[46] G. King, A.M. Abakumov, J. Hadermann, A.M. Alekseeva, M.G. Rozova, T. Perkisas, P.M. Woodward, G. van Tendeloo, E.V. Antipov, Inorg. Chem. 49 (2010) 6058.
[47] L.M. Kovba, L.N. Lykova, M.V. Paromova, N.N. Schevchenko, Zh. Neorg. Khim. 18 (1973) 835.
[48] D. Reinen, H. Weitzel, Z. Anorg. Allg. Chem. 424 (1976) 31.
[49] J. Wang, B.H. Toby, P.L. Lee, L. Ribaud, S.M. Antao, C. Kurtz, M. Ramanathan, R.B. von Dreele, M.A. Beno, Rev. Sci. Instrum. 79 (2008) 085105.
[50] P.L. Lee, D. Shu, M. Ramanathan, C. Preissner, J. Wang, M.A. Beno, R.B. von Dreele, L. Ribaud, C. Kurtz, S.M. Antao, X. Jiao, B.H. Toby, J. Synchr. Radiat. 15 (2008) 427.
[51] B.H. Toby, Y. Huang, D. Dohan, D. Caroll, X. Jiao, L. Ribaud, J.A. Doebbler, M.R. Suchomel, J. Wang, C. Preissner, D. Kline, T.M. Mooney, J. Appl. Cryst. 42 (2009) 990.
[52] V. Favre-Nicolin, R.J. Černy, J. Appl. Cryst. 35 (2002) 734.
[53] A.C. Larson, R.B. von Dreele, General Structure Analysis System (GSAS), Los Alamos National Laboratory Report LAUR 86-748, 2000.
[54] B.H. Toby, J. Appl. Cryst. 34 (2001) 210.
[55] G. Blasse, J. Inorg. Nucl. Chem. 27 (1965) 993.
[56] M. Gateshki, J.M. Igartua, E. Hernández-Bocanegra, J. Phys. Condens. Matter 15 (2003) 6199.